CAPNOGRAPHIC PARAMETERS IN VENTILATED PATIENTS: CORRESPONDENCE WITH AIRWAY AND LUNG TISSUE MECHANICS

1. Zsofia Csorba, MD
Affiliation: Department of Anesthesiology and Intensive Therapy, University of Szeged, Hungary
Email: drcsorbazsofia@gmail.com
Role: This author helped conduct the study and analyze the data
Conflicts: Zsofia Csorba reported no conflicts of interest
Attestation: Zsofia Csorba has seen the original study data, reviewed the analysis of the data, and approved the final manuscript

2. Ferenc Petak, PhD
Affiliation: Department of Medical Physics and Informatics, University of Szeged, Hungary
Email: petak.ferenc@med.u-szeged.hu
Role: This author helped design the study, conduct the study, analyze the data, and write the manuscript
Conflicts: Ferenc Petak reported no conflicts of interest
Attestation: Ferenc Petak has seen the original study data, reviewed the analysis of the data, and approved the final manuscript, and is the author responsible for archiving the study files

3. Kitti Nevery
Affiliation: Department of Anesthesiology and Intensive Therapy, University of Szeged, Hungary
Email: neverykitti@gmail.com
Role: This author helped conduct the study and analyze the data
Conflicts: Kitti Nevery reported no conflicts of interest
Attestation: Kitti Nevery has seen the original study data and approved the final manuscript

4. Jozsef Tolnai, PhD
Affiliation: Department of Medical Physics and Informatics, University of Szeged, Hungary
Email: tolnai.jozsef@med.u-szeged.hu
Role: This author helped conduct the study and analyze the data
Conflicts: Jozsef Tolnai reported no conflicts of interest
Attestation: Jozsef Tolnai has seen the original study data and approved the final manuscript

5. Adam L. Balogh, MD
Affiliation: Department of Anesthesiology and Intensive Therapy, University of Szeged, Hungary
Email: balogh.adam.laszlo@med.u-szeged.hu
Role: This author helped conduct the study and analyze the data
Conflicts: Adam L. Balogh reported no conflicts of interest
Attestation: Adam L. Balogh has seen the original study data and approved the final manuscript

6. **Ferenc Rarosi**
Affiliation: Department of Medical Physics and Informatics, University of Szeged, Hungary
Email: rarosi.ferenc@med.u-szeged.hu
Role: This author helped analyze the data
Conflicts: Ferenc Rarosi reported no conflicts of interest
Attestation: Ferenc Rarosi has seen the original study data and approved the final manuscript

7. **Gergely H Fodor, MD**
Affiliation: Department of Medical Physics and Informatics, University of Szeged, Hungary
Email: fodor.gergely@med.u-szeged.hu
Role: This author helped analyze the data
Conflicts: Gergely H Fodor reported no conflicts of interest
Attestation: Gergely H Fodor has seen the original study data and approved the final manuscript

8. **Barna Babik, MD, PhD**
Affiliation: Department of Anesthesiology and Intensive Therapy, University of Szeged, Hungary
Email: babikbarna@gmail.com
Role: This author helped design the study, conduct the study, analyze the data, and write the manuscript
Conflicts: Barna Babik reported no conflicts of interest
Attestation: Barna Babik has seen the original study data, reviewed the analysis of the data, and approved the final manuscript

Institution: Department of Anesthesiology and Intensive Therapy, Department of Medical Physics and Informatics, University of Szeged
Short Title: Capnography in ventilated patients
Funding: Funded by a Hungarian Basic Research Grant (OTKA K81179). This research was supported by the European Union and the State of Hungary, co-financed by the European Social Fund in the framework of TÁMOP 4.2.4. A/2-11-1-2012-0001 'National Excellence Program'.

Corresponding Author:
Ferenc Petak, PhD
Department of Medical Physics and Informatics
Korányi fasor 9, Hungary H-6720
Phone: +36 62 545077
FAX: +36 62 545077
Email: petak.ferenc@med.u-szeged.hu

Submitted as a **Research Report**

This report describes human research. IRB contact information: Regional and Institutional Human Medical Biological Research Ethics Committee H-6720 Szeged, Korányi fasor 8-10.
Tel. +36 62 545997, e-mail: kutetika@gmail.com

ABSTRACT

Background: Although the mechanical status of the lungs affects the shape of the capnogram, the relationships between the capnographic parameters and those reflecting the airway and lung tissue mechanics have not been established in mechanically ventilated patients. We therefore set out to characterize how the mechanical properties of the airways and lung tissues modify the indices obtained from the different phases of the time and volumetric capnograms, and how the lung mechanical changes are reflected in the altered capnographic parameters after a cardiopulmonary bypass (CPB).

Methods: Anesthetized, mechanically ventilated patients (n=101) undergoing heart surgery were studied in a prospective consecutive cross sectional study under the open-chest condition before and 5 min after CPB. Forced oscillation technique was applied to measure airway resistance (Raw), tissue damping (G) and elastance (H). Time and volumetric capnography were performed to assess parameters reflecting the phase II (S_{II}) and III slopes (S_{III}), their transition (D_{2min}), the dead-space indices according to Fowler, Bohr and Enghoff and the intrapulmonary shunt.

Results: Before CPB, S_{II} and D_{2min} exhibited the closest ($p=0.006$) associations with H (0.65 and -0.57; $p<0.0001$, respectively), whereas S_{III} correlated most strongly ($p<0.0001$) with Raw ($r=0.63$; $p<0.0001$). CPB induced significant elevations in Raw and G and H ($p<0.0001$). These adverse mechanical changes were reflected consistently in S_{II}, S_{III} and D_{2min}, with weaker correlations with the dead-space indices ($p<0.0001$). The intrapulmonary shunt expressed as the difference between the Enghoff and Bohr dead-space parameters was increased after CPB (95±5[SEM]% vs. 143±6%; $p<0.001$).

Conclusions: In mechanically ventilated patients, the capnographic parameters from the early phase of expiration (S_{II} and D_{2min}) are linked to the pulmonary elastic recoil, while the effect of airway patency on S_{III} dominates over the lung tissue stiffness. However, severe deteriorations in lung resistance or elastance affects both capnogram slopes.

Word count: 294

INTRODUCTION

The capnogram is a curve reflecting the concentration change of carbon dioxide (CO_2) as an endogenous indicator during expiration. In addition to verifying the correctness of the airway management, capnography provides information about the uniformity of lung emptying and adverse changes in the overall airway geometry (1-8) and respiratory tissue stiffness (6-8), and it serves as a valuable tool for the recognition of pulmonary circulatory abnormalities (9-11). International recommendations for standards require the monitoring of ventilation with capnography in all patients undergoing sedation or general anesthesia (12,13).

Characterization of the relationships between standard lung function parameters and capnographic indices provides a valuable tool facilitating an understanding of the various shapes of the capnogram (1,2,14). However, the earlier studies demonstrating associations between the capnographic slope factors with the forced expiratory volume in 1 s (FEV_1) (1,14) and the peak expiratory flow (2,14) were limited to spontaneously breathing subjects. Despite the particular importance of recognizing adverse alterations in the pulmonary system in mechanically ventilated patients, details as to how the resistive and/or elastic properties of the pulmonary system affect the various indices derived from the capnogram are essentially lacking from the literature. In the present study, therefore, we set out to establish the connections between the various phase, shape, dead-space or pulmonary shunt circulation parameters of the time or volumetric capnogram and those reflecting the airway and lung tissue mechanics, expiratory flow and gas exchange. In order to gain an insight into within-subject alterations in the pulmonary condition, a large cohort of ventilated patients were examined during cardiac surgery, a cardiopulmonary bypass (CPB) being applied to generate a temporary complex realignment in the pulmonary mechanics and circulation.

METHODS

Detailed description of the patients' characteristics, methodology and results can be found in an online supplement.

Patients

After they have provided their written informed consent, 101 patients (female/male: 30/71, 62±9 yrs) undergoing elective open heart surgeries were examined in a prospective, consecutive cross sectional manner. The study protocol was approved by the Human Research Ethics Committee of Szeged University, Hungary (no. WHO 2788). Patients were excluded in the event of severe cardiopulmonary disorders (pleural effusion >300 ml, ejection fraction <30%, BMI >35 kg/m^2 or intraoperative acute asthma exacerbation).

Anesthesia and surgery

Intravenous midazolam (30 μg/kg), sufentanil (0.4-0.5 μg/kg) and propofol (0.3-0.5 mg/kg) were applied to induce anesthesia. The maintenance of anesthesia and muscle relaxation was ensured by an intravenous infusion of propofol (50 μg/kg/min) and intravenous boluses of rocuronium (0.2 mg/kg every 30 min).

Endotracheal intubation was performed and the patients were mechanically ventilated in volume-controled mode with descending flow (Dräger Zeus, Lübeck, Germany). The tidal volume was set to 7 ml/kg with a ventilator frequency of 9-14 breaths/min, a positive end-expiratory pressure (PEEP) of 4 cmH_2O, and an inspired oxygen fraction of (FiO_2) of 0.5. Arterial blood gas samples were analyzed to calculate the Horowitz coefficient ($HQ=P_{aO_2}/FiO_2$). During cardioplegic cardiac arrest, the lungs were not ventilated with

maintaining no positive airway pressure. The lungs were then inflated 3-5 times to a peak airway pressure of 30 cmH_2O before declamping of the aorta to perform lung recruitment.

Forced oscillatory measurements

The low-frequency forced oscillation technique was applied to measure the lung mechanical properties, as detailed previously (15). The volume history was standardized by inflating the lungs to a pressure of 30 cmH_2O before the oscillatory measurements. Forced oscillatory signal was introduced into the lungs during short (15-s) apneic periods. The input impedance of the lung (ZL) was computed from the power spectra of the airway opening pressure and tracheal airflow. A model (16) containing a frequency-independent airway resistance (Raw) and inertance (Iaw) and a constant-phase tissue compartment characterized by the coefficients of damping (G) and elastance (H) was fitted to the mean ZL data. The lung tissue resistance (Rti) and the total lung resistance (RL) at the ventilation frequency (0.2 Hz) was also calculated from the ZL spectra.

Recording and analyses of the expiratory capnogram

A mainstream capnograph (Novametrix, Capnogard®, Andover, MA, USA) and another central airflow meter (Piston Ltd., Budapest, Hungary) were connected into the ventilatory circuit at the Y-piece, and 15-s CO_2 and ventilator flow traces were recorded simultaneously. The CO_2 and ventilator flow traces were digitized and imported into custom-made signal analysis software. The slopes of phase III of the capnogram in the time ($S_{III,T}$) and in the volumetric ($S_{III,V}$) domains were determined by fitting a linear regression line to the last two-thirds of each phase-III traces (Fig. 1) (17,18). The phase-II slopes of the time ($S_{II,T}$) and volumetric ($S_{II,V}$) capnograms were determined by calculating the slopes of the best-fitting line around the inflection point (±20%). Each slope was divided by the average corresponding CO_2

concentration in the mixed expired gas to obtain normalized time ($S_{nII,T}$ and $S_{nIII,T}$) and volumetric ($S_{nII,V}$ and $S_{nIII,V}$) phase-II and III slopes (19-21). This normalization was made only for the slope indices, as performed earlier before and after CPB (11). The angle (α_{cap}) formed by the phase-II and III limbs of the expiratory time capnogram was also calculated by using a standard monitoring speed of 12.5 mmHg/s. The transition rates of change from phase II to phase III in the time (D_{2min}) and volumetric (D_{2Vmin}) capnograms reflecting the curvature were calculated as the minima of the second-order time and volumetric derivatives (22).

Besides these shape factors, dead-space parameters were derived from the volumetric capnograms. The Fowler dead-space (V_{DF}), reflecting the anatomic dead-space volume of the conducting airways was determined by calculating the expired gas volume until the inflection point of phase II was reached in the volumetric capnogram (23,24). The physiological dead-space, including also the alveolar volume not involved in gas exchange, was assessed by the Bohr method (V_{DB}) (25). The dead-space according to Enghoff's modification (V_{DE}) was calculated; this takes also into account the not ventilated, but still perfused alveoli (26).

We also calculated the differences between the Enghoff and Bohr dead-space parameters (V_{DE} - V_{DB}) representing the pulmonary shunt circulation. The intrapulmonary shunt blood flow (Qs/Qt) was additionally assessed via the Fick equation.

Under both experimental conditions, 3 to 5 expiratory traces in each recording were analyzed, resulting in the ensemble-averaging of 10-12 values for further analysis in each patient.

Analysis of the expiratory flow

To characterize the expiratory flow pattern, the expiratory phases of each V' recordings were analyzed by fitting an exponential function to the elevating limb (27):

$$V'(t) = V'_{pl} - PF \cdot e^{-LF \cdot t}$$

where V'_{pl} is the plateau flow before the beginning of the next inspiration, PF is the peak expiratory flow, and LF is related to the curvature of the expiratory curve. The parameter LF is related to the curvature of the expiratory curve; a larger value indicates a more concave shape in the late flow. Model fitting to the serial data points from the peak flow was performed until 90% of the equilibrium value of V'(t) was reached.

Measurement protocol

Two sets of measurements were made under the open-chest condition 5 min before the CPB and 5 min after the patient was weaned from the CPB. Recruitment maneuvers were performed before the weaning from the CPB. Each data collection period started with recordings of 3 to 5 capnogram traces. During this period, an arterial blood gas sample was taken to measure P_{aO_2} and P_{aCO_2} for the calculation of HQ and V_{DE}, respectively. The total lung resistance (R_{vent}) and compliance (C_{vent}) displayed by the respiratory monitor of the ventilator were registered at this stage of the protocol. The data collections under both conditions were supplemented by recordings of 3 to 5 ZL data epochs at 1-min intervals.

Data analyses

Sample size estimation was applied to involve sufficient number of patients for the detection of clinically relevant significances. The type 1 error rate was set to 0.05, the statistical power was

set to 0.85 and the clinically relevant effect size (alternative hypothesis) was considered to detect correlation coefficients r=0.3 versus r=0. The necessary sample size was 96.

Scatters in measured variables are expressed as SEM values. In the event of passing the normality test (marked in footnotes), paired t-tests were used to examine the statistical significance of the changes induced in the parameters by the CPB. Wilcoxon signed-rank tests were applied otherwise to verify the significance of the changes in the mechanical, capnographic or gas exchange parameters. The Pearson test was applied to analyze the correlations between the different variables. The comparison of Pearson correlation coefficients were made by Steiger's Z-test; these tests were performed between the particular and the nearest r values. Subgroups of patients were formed based on the initial HQ level (high and low 25 percentile), and based on the extremity of changes after surgery (top 25 percentile increase and bottom 25 percentile decrease in HQ, respectively). Time domain capnogram slope indices and Raw and C_{vent} and their changes after the surgery were also correlated in these subgroups and were compared to the results obtained from the pooled population. Values $p<0.05$ were considered to be statistically significant.

RESULTS

Parameters reflecting the lung mechanics and the expiratory flow are demonstrated in Fig. 2. All the resistive parameters including those reflecting the flow resistance of the airways (Raw) or of the lung tissues (Rti) or the combination of these compartments (R_{vent} and RL), exhibited marked and statistically significant increases after CPB ($p<0.0001$ for each). Conversely, more moderate, but still highly significant decreases were observed following CPB in the compliance parameters determined at end-expiratory lung volume by the oscillometry (CL) or at end-inspiratory lung volume by the ventilator (C_{vent}) ($p<0.0001$ for both). CPB induced no statistically detectable changes in PF ($p=0.5$), whereas the parameter LF, reflecting the curvature of the late flow, increased significantly ($p<0.0001$). The CPB-induced adverse lung mechanical changes were also reflected in the significant decrease in HQ (from 371±11 to 350±14 mmHg; $p=0.038$[1]).

Figure 3 depicts the indices derived from the time and volumetric capnographic measurements before and after the CPB. Marked and statistically significant increases were observed in the time and volumetric parameters reflecting the phase-III slope of the expired CO_2 ($p<0.0001$ for $S_{III,T}$, $S_{nIII,T}$, $S_{III,V}$ and $S_{nIII,V}$) after the CPB. The slopes of phase II revealed significant decreases following CPB ($p<0.0001$ for both $S_{II,T}$ and $S_{II,V}$), whereas these drops were no longer detectable after normalization to the CO_2 concentration in the mixed expired gas ($p=0.4$ and 0.9 for $S_{nII,T}$ and $S_{nII,V}$, respectively[1]). CPB increased the curvature representing the transition from phase II to phase III ($p<0.0001$ for both D_{2min} and D_{2Vmin}). Uniform decreases were detected in V_{DF} and V_{DB} ($p<0.0001$) after the CPB, whereas V_{DE} increased significantly ($p<0.0001$). These changes in the dead-space parameters resulted in significant elevations in the shunt parameters

[1] Shapiro-Wilk test for normality passed ($p>0.41$)

reflecting the alterations in lung ventilation ($p=0.02$ and $p<0.0001$ for V_{DB} - V_{DF} and V_{DE} - V_{DB}, respectively[2]) and perfusion (Qs/Qt, $p<0.0001$).

Figure 4 illustrates the strengths of the correlations between the lung mechanical parameters (x-axis) and the time and volumetric capnographic parameters reflecting the slopes, transitions, dead-space and shunt fractions (y-axis).

The lung resistive parameters exhibited the closest associations with the phase-III slope capnographic parameters ($p<0.0001$), particularly after the CPB, when all the indices reflecting the resistive properties of the pulmonary system were markedly elevated ($p<0.0001$; Fig. 4, top panels). Significant, but somewhat weaker correlations were observed between the lung resistive parameters and the ventilation dead-space parameters V_{DF} ($p<0.0001$) and V_{DB} ($p<0.0001$). More specifically, the mechanical parameter representing the flow resistance of the airways (Raw) correlated best ($p<0.0001$) with the $S_{III,T}$ ($r=0.63$ and 0.68 for $S_{III,T}$ before and after the CPB, respectively; $p<0.0001$). Moreover, Raw correlated significantly with $S_{III,V}$ ($r=0.43$ and 0.55 for $S_{III,V}$ before and after CPB, respectively, $p<0.0001$). Normalization of the phase-III slopes to the CO_2 concentration in the mixed expired gas did not affect these relationships noticeably ($p=0.71$). Conversely, the mechanical parameters characterizing lung tissue elasticity (H and C_{vent}) showed the closest ($p=0.006$) relationships with the time capnographic parameters describing the phase II ($r=0.65$ and 0.41 between H and $S_{II,T}$ before and after the CPB, respectively; $p<0.0001$). The pulmonary elastance and compliance parameters also revealed close associations with the capnographic indices reflecting the curvatures of the transitions between the phases, particularly before the CPB ($r=-0.57$ between H and D_{2min}; $p<0.0001$). The early and late-phase expiratory flow parameters revealed strong

[2] Shapiro-Wilk test for normality passed ($p>0.13$)

associations between PF and the dead-space indices both before and after the CPB. LF exhibited the strongest correlation with $S_{nIII,V}$ (r=0.53; p<0.0001).

As concerns the relationships between the CPB-induced changes in the lung mechanical and capnographic indices (Fig. 4, bottom panel), the marked elevations in Raw correlated best (p=0.001) with the decreases in the phase-II slope parameters of the time capnogram (r=-0.72 and -0.70 for $S_{II,T}$ and $S_{nII,T}$, respectively; p<0.0001). The CPB-induced airway narrowing was also reflected in the elevated phase-III slope parameters of the time and volumetric capnograms (r=0.49 for both $S_{III,T}$ and $S_{III,V}$; p<0.0001), and the curvature of the transition between the phases in the time domain (r=0.6 for D_{2min}; p<0.0001). The changes in the other mechanical parameters reflecting the tissue (G) or total lung resistance (RL or R_{vent}) displayed similar relationships with the alterations in the various capnographic indices after the CPB. Assessment of the mild CPB-induced stiffening of the lung tissue also revealed statistically significant correlations between the changes in C_{vent} and those in the phase-III slope parameters in both the time and volumetric capnograms (r=-0.48 for both $S_{nIII,T}$ and $S_{nIII,V}$; p<0.0001). Neither the absolute values of HQ nor the changes following CPB exhibited close relationships with any other mechanical or capnographic indices; an association was observed with V_{DE} before the CPB (r=0.31; p<0.0002).

The relationships between the initial fundamental lung mechanical and capnographic indices for the subgroups of patients based on starting HQ are depicted on Fig. 5A. Strong positive significant correlations were observed between Raw and phase III slope parameters (p=0.002) and between C_{vent} and phase II slope parameters independently of the subgroup allocation (p=0.001). The initial C_{vent}-$S_{III,T}$ relationship was not significantly correlated (p=0.20), while the Raw-$S_{II,T}$ correlation appeared significant only for the pooled patient population (p=0.0045). The changes in Raw correlated to those in both slope variables (p<0.0001), whereas

the alterations in C_{vent} were significantly related with those in phase III slopes ($p=0.023$, Fig. 5B).

Findings reflecting interindividual variability and demonstrating individual changes are included in the online supplement (Table 1S and Fig. 1S). A large range was obtained for the coefficient of variation in the initial lung mechanical and capnograpm parameters (ranging from 25% to 169% for V_{DB} and $S_{nIII,T}$, respectively). Further interdependences of the main capnogram shape factors and lung mechanical parameters are illustrated in Fig. 2S in the online supplement.

DISCUSSION

Capnography is an essential part of the monitoring in patients requiring mechanical ventilation. The present study was motivated to elucidate how changes in the mechanical properties of the different lung compartments are reflected in the alterations in the shape, dead-space and pulmonary shunt circulation parameters obtained from the time or volumetric capnograms. A detailed characterization of the airway and lung tissue mechanics was combined with a comprehensive evaluation of the capnographic indices before and after a lung function deterioration induced by a CPB. Our study revealed the specific influence of the lung resistive and elastic parameters on the capnogram shape indices in ventilated patients.

Phase-III slope

The results demonstrated significant increases in both $S_{III,T}$ and $S_{III,V}$ immediately following the CPB. The elevations also appeared after normalization to the CO_2 concentration in the mixed expired gas (11) (Fig. 3). This finding differs from that observed previously in a smaller cohort of ventilated cardiac surgery patients, where no major changes were observed in the phase-III slope after CPB (11). The discrepancy may be attributed to the more aggressive maneuvers applied to recruit the lungs after the CPB in this earlier study, to the application of a higher PEEP (7 vs. 4 cmH_2O) and to the somewhat delayed measurement time after the CPB (15 min vs. 5 min).

The phase-III slope of the capnogram is considered to reflect the summation of the ventilation inhomogeneities relating to the working alveolar compartments with different time constants and the ventilation-perfusion mismatch as concerns the dead-space and/or intrapulmonary shunt. The overall and the regional lung emptying are determined by the opposite effects of Raw, G and the lung recoil tendencies (6). The role of the lung tissue stiffness decreases dynamically toward the end of expiration, and the elastic recoil affects S_{III} in patients with low

or high compliance (6). Raw, therefore, exerted the primary influence on the S_{III} parameters before the CPB (Figs 4 and 1S), independent from the initial lung function (i.e. HQ; Fig. 5A). This finding is in accord with the postulate of the close link between the airway cross-sectional area and S_{III}, based on spirometric data obtained previously in spontaneously breathing patients (1,3,28). Representing (G) or incorporating lung parenchymal resistive component (RL and R_{vent}) weakened the correlation substantially ($p<0.0001$; Fig. 4). This suggests that under baseline conditions the internal friction in the lung tissue does not exert a major effect on the capnographic S_{III} indices, along with the lesser role of compliance. Following the CPB, significant associations appeared between the overall resistive and capnographic phase-III slope parameters, due to the greatly elevated tissue resistance (Fig. 4). Thus, an elevated S_{III} may indicate the presence of lung disorders affecting not only the airways, but also the tissue resistive properties, such as observed during interstitial edema in sepsis or cardiac failure (29). These phenomena are comprehensively confirmed by the significantly elevated concavity of the late expiratory flow (Fig. 2), the increase in V_{DE} and the diminished HQ (Fig. 3).

Phase-II slope

The phase-II slope was decreased following the CPB in both the time and the volumetric capnograms. This agrees with the results of the only earlier study, where the changes in S_{II} were measured 2 min after establishment of the full pulmonary blood flow (11). However, normalization of S_{II} to a possible lower CO_2 content of the expired gas (i.e. S_{nII}) after weaning from the CPB eliminated these changes (Fig. 3), because the intensity of axial gas mixing depends on the CO_2 concentration (11).

Phase II of the capnogram represents the overall width of the moving airway-alveolar gas front and its slope may be explained by opposing effects. The heterogeneous start of lung emptying, the reduced airway lumen and increased tissue damping may all contribute to the decreases,

whereas an elevated elastic recoil and a low alveolar CO_2 content may counteract these changes in S_{II} (1,3,11,30). Before the CPB, the correlation analyses of the S_{II} parameters indicated their close relationship with the elastic properties of the lungs (Fig. 4), independent from the starting gas exchange ability of the lungs (Fig. 5A). This finding is in accordance with a wider phase II observed previously in emphysematous patients (31,32), and increases in S_{II} after compliance elevation through recruitment maneuvers (30). Since PF is determined more by the lung tissue stiffness ($r=0.34$; $p<0.0001$ for H) than by the airway caliber ($r=0.09$; $p=0.34$ for Raw), the significant correlation of PF with the phase-II capnographic indices may also be attributed to the influence of the lung elastance during early expiration.

Independent of the direction and magnitude of change in HQ, the CPB-induced changes in S_{II} exhibited close correlations with the markedly elevated Raw (Fig. 5B) and lung resistance parameters (RL and R_{vent}; Fig. 4). This finding indicates that inhomogeneous airway constriction leads to a more sequential emptying of lung compartments with different CO_2 content even at the beginning of expiration, and thereby widens the airway-alveolar gas front with subsequent decreases in the phase-II slope. The loss of correlations between the changes in $S_{II,T}$ and C_{vent} (Fig. 5B) may be due to the complex and opposing phenomena affecting $S_{II,T}$, as described earlier.

Capnographic parameters reflecting phase transitions

The transition indices (α_{cap}, D_{2min} and D_{2Vmin}) reside in the same part of the capnogram, but their meanings are different. α_{cap} is the angle between S_{II} and S_{III}, i.e. the relationship between the overall gas front and the alveolar gas volume, while D_{2min} and D_{2Vmin} are related to the internal surface of the moving CO_2 diffusion front in the airways during expiration. The elevation observed in α_{cap} after the CPB reflects the combined alterations in S_{II} and S_{III}, whereas both second derivative parameters approached zero after the CPB (Fig. 3), demonstrating

blunted (less cornered) transitions between capnographic phases II and III. This finding may be attributed to the highly heterogeneous severe airway constriction that developes after the CPB, which blurs the resulting diffusion front measured in the central airway. The close associations between FEV_1 and the capnographic indices reflecting the phase-II to phase-III transition in spontaneously breathing patients is in accordance with this result (1). Our data further demonstrate that, in ventilated patients, the low compliance associated with the normal airway patency compresses the flow profile, resulting in a sharper phase-II to phase-III transition (Fig. 1S, C). This finding reveals the sensitivity of D_{2min} and D_{2Vmin} parameters to changes in lung compliance as opposed to α_{cap}, which demonstrates rather resistive properties (Fig. 4).

Dead-space and shunt parameters

The anatomical dead space (V_{DF}) was decreased slightly but consistently after the CPB (Fig. 3). Since this change was associated with marked increases in Raw and LF (Fig. 4, bottom), the compromised lumen of the conducting airways and/or their exclusion from the ventilation may explain this finding. The dead-space parameter incorporating the additional volume of the unperfused alveoli (V_{DB}) followed very similar changing and correlation patterns, indicating the negligible unperfused, but ventilated alveolar compartment after the CPB. The bronchoconstriction resulting from the additive effects of SIRS and local hypocapnia may contribute to the low alveolar dead-space. Conversely, supine position, surgery and CPB led to elevations in V_{DE} (Fig. 3), suggesting a substantial enlargement of the volume of the not ventilated but perfused alveoli due to persistent atelectasis after the CPB (33,34).

The difference between V_{DE} and V_{DB}, which approximates the extent of the pulmonary shunt, was increased markedly after the CPB (Fig. 3). It is noteworthy that V_{DE} - V_{DB} exhibited parallel changes and a significant correlation ($r=0.47$; $p<0.0001$) with the shunt fraction obtained from

the classical shunt equation (Qs/Qt), highlighting the additional usefulness of volumetric capnography in the assessment of the intrapulmonary shunt (Fig. 3).

Methodological aspects

While patients with severe cardiopulmonary disorders were excluded from the present study, the pulmonary status of the participating subjects varied widely from relatively healthy lungs to obstructive and restrictive disorders. Such interindividual variety of pulmonary symptoms with additional demographic and anthropometric differences are expected to occur in all health-care units providing ventilatory support. Therefore, this feature of the study is particularly favorable and also facilitates the performance of the correlation analyses.

It is also noteworthy that the results represent an open chest condition. Significant alteration in lung-thorax dynamics is expected to influence both the capnography indices and forced oscillatory data reflecting airway and tissue mechanics (35). The capnogram parameters are determined by the heterogeneity of the lungs, geometry of the airway tree and the forces exerted by the tissue resistive and elastic properties of the lungs and the chest wall (6). While our study allows an insight into the mechanisms coupling the capnogram and mechanical parameters, a further study in intact chest patients may be needed to generalize our findings.

A further important methodological aspect of the present study is related to the use of correlation analyses to assess the associations between parameters obtained by two different techniques. As a general rule, the existence of significant correlations between variables is necessary, but not sufficient to imply a causal relationship. In the present study, the lung mechanical and capnographic parameters are linked to each other through local common mechanisms governing lung emptying. Furthermore, the individual correlation results from consistent physiological and clinical findings. These considerations verify that causation can be inferred with great certainty.

Summary and conclusions

In conclusion, we characterized the relationships between the time or volumetric capnographic parameters and the lung mechanical indices reflecting the airway and the lung tissue viscoelastic properties in cardiac surgery patient underwent open heart surgery. The lung tissue stiffness predominantly determines the capnographic parameters in the early phase of expiration, since the elastic forces are maximal at high lung volumes. Thus, in the vast majority of the cases, the phase-II slope of the capnogram is predominantly determined by pulmonary elastic recoil. Conversely, the resistive properties of the lungs become increasingly important during the later phase of expiration and thus, the phase-III slope is shaped overwhelmingly by the airway resistance. However, markedly elevated lung resistance additionally worsens the capnogram phase II slope. Similarly, severely compromised lung elastance also distorts the capnogram phase III slope. Since computational methods could be incorporated into the modern anesthesia machines to quantify capnographic shape factors, these parameters together with the traditional bedside mechanical indices has the promise to improve differential diagnoses and advance guiding respiratory therapy.

REFERENCES

1. You B, Peslin R, Duvivier C, Vu VD, Grilliat JP. Expiratory capnography in asthma: evaluation of various shape indices. The European respiratory journal 1994;7:318-23.
2. Yaron M, Padyk P, Hutsinpiller M, Cairns CB. Utility of the expiratory capnogram in the assessment of bronchospasm. Annals of emergency medicine 1996;28:403-7.
3. Krauss B. Capnography as a rapid assessment and triage tool for chemical terrorism. Pediatric emergency care 2005;21:493-7.
4. Stromberg NO, Gustafsson PM. Ventilation inhomogeneity assessed by nitrogen washout and ventilation-perfusion mismatch by capnography in stable and induced airway obstruction. Pediatric pulmonology 2000;29:94-102.
5. Blanch L, Romero PV, Lucangelo U. Volumetric capnography in the mechanically ventilated patient. Minerva anestesiologica 2006;72:577-85.
6. Babik B, Csorba Z, Czovek D, Mayr PN, Bogats G, Petak F. Effects of respiratory mechanics on the capnogram phases: importance of dynamic compliance of the respiratory system. Critical care 2012;16:R177.
7. Romero PV, Lucangelo U, Lopez Aguilar J, Fernandez R, Blanch L. Physiologically based indices of volumetric capnography in patients receiving mechanical ventilation. The European respiratory journal 1997;10:1309-15.
8. Yang Y, Huang Y, Tang R, Chen Q, Hui X, Li Y, Yu Q, Zhao H, Qiu H. Optimization of positive end-expiratory pressure by volumetric capnography variables in lavage-induced acute lung injury. Respiration; international review of thoracic diseases 2014;87:75-83.
9. Chopin C, Fesard P, Mangalaboyi J, Lestavel P, Chambrin MC, Fourrier F, Rime A. Use of capnography in diagnosis of pulmonary embolism during acute respiratory failure of chronic obstructive pulmonary disease. Critical care medicine 1990;18:353-7.
10. Verschuren F, Liistro G, Coffeng R, Thys F, Roeseler J, Zech F, Reynaert M. Volumetric capnography as a screening test for pulmonary embolism in the emergency department. Chest 2004;125:841-50.
11. Tusman G, Areta M, Climente C, Plit R, Suarez-Sipmann F, Rodriguez-Nieto MJ, Peces-Barba G, Turchetto E, Bohm SH. Effect of pulmonary perfusion on the slopes of single-breath test of CO2. Journal of applied physiology 2005;99:650-5.

12. Merry AF, Cooper JB, Soyannwo O, Wilson IH, Eichhorn JH. International Standards for a Safe Practice of Anesthesia 2010. Canadian journal of anaesthesia = Journal canadien d'anesthesie 2010;57:1027-34.
13. Guidelines for Patient Care in Anesthesiology. http://www.asahq.org/resources/standards-and-guidelines: American Society of Anesthsiologists, 2011.
14. Veronez L, Pereira MC, da Silva SM, Barcaui LA, De Capitani EM, Moreira MM, Paschoal IA. Volumetric capnography for the evaluation of chronic airways diseases. International journal of chronic obstructive pulmonary disease 2014;9:983-9.
15. Babik B, Asztalos T, Petak F, Deak ZI, Hantos Z. Changes in respiratory mechanics during cardiac surgery. Anesthesia and analgesia 2003;96:1280-7, table of contents.
16. Hantos Z, Daroczy B, Suki B, Nagy S, Fredberg JJ. Input impedance and peripheral inhomogeneity of dog lungs. Journal of applied physiology 1992;72:168-78.
17. Krauss B, Deykin A, Lam A, Ryoo JJ, Hampton DR, Schmitt PW, Falk JL. Capnogram shape in obstructive lung disease. Anesth Analg 2005;100:884-8, table of contents.
18. Blanch L, Lucangelo U, Lopez-Aguilar J, Fernandez R, Romero PV. Volumetric capnography in patients with acute lung injury: effects of positive end-expiratory pressure. Eur Respir J 1999;13:1048-54.
19. Ream RS, Schreiner MS, Neff JD, McRae KM, Jawad AF, Scherer PW, Neufeld GR. Volumetric capnography in children. Influence of growth on the alveolar plateau slope. Anesthesiology 1995;82:64-73.
20. Tusman G, Areta M, Climente C, Plit R, Suarez-Sipmann F, Rodriguez-Nieto MJ, Peces-Barba G, Turchetto E, Bohm SH. Effect of pulmonary perfusion on the slopes of single-breath test of CO2. J Appl Physiol 2005;99:650-5.
21. Tsoukias NM, Tannous Z, Wilson AF, George SC. Single-exhalation profiles of NO and CO2 in humans: effect of dynamically changing flow rate. J Appl Physiol 1998;85:642-52.
22. Ioan I, Demoulin B, Duvivier C, Leblanc AL, Bonabel C, Marchal F, Schweitzer C, Varechova S. Frequency dependence of capnography in anesthetized rabbits. Respiratory physiology & neurobiology 2014;190:14-9.
23. Fowler WS. Lung function studies; the respiratory dead space. The American journal of physiology 1948;154:405-16.
24. Fowler WS. Respiratory dead space. Federation proceedings 1948;7:35.
25. Bohr C. Über die Lungenatmung. Skan Arch Physiol 1891;53:236-8.

26. Enghoff H. Volumen inefficax. Uppsala Laekareforen Forh 1938;44:191-218.
27. van Drunen EJ, Chiew YS, Chase JG, Shaw GM, Lambermont B, Janssen N, Damanhuri NS, Desaive T. Expiratory model-based method to monitor ARDS disease state. Biomedical engineering online 2013;12:57.
28. Nik Hisamuddin NA, Rashidi A, Chew KS, Kamaruddin J, Idzwan Z, Teo AH. Correlations between capnographic waveforms and peak flow meter measurement in emergency department management of asthma. International journal of emergency medicine 2009;2:83-9.
29. Dellaca RL, Zannin E, Sancini G, Rivolta I, Leone BE, Pedotti A, Miserocchi G. Changes in the mechanical properties of the respiratory system during the development of interstitial lung edema. Respiratory research 2008;9:51.
30. Tusman G, Bohm SH, Suarez-Sipmann F, Turchetto E. Alveolar recruitment improves ventilatory efficiency of the lungs during anesthesia. Canadian journal of anaesthesia = Journal canadien d'anesthesie 2004;51:723-7.
31. Kars AH, Bogaard JM, Stijnen T, de Vries J, Verbraak AF, Hilvering C. Dead space and slope indices from the expiratory carbon dioxide tension-volume curve. The European respiratory journal 1997;10:1829-36.
32. Schwardt JD, Neufeld GR, Baumgardner JE, Scherer PW. Noninvasive recovery of acinar anatomic information from CO2 expirograms. Annals of biomedical engineering 1994;22:293-306.
33. Tenling A, Hachenberg T, Tyden H, Wegenius G, Hedenstierna G. Atelectasis and gas exchange after cardiac surgery. Anesthesiology 1998;89:371-8.
34. Verheij J, van Lingen A, Raijmakers PG, Spijkstra JJ, Girbes AR, Jansen EK, van den Berg FG, Groeneveld AB. Pulmonary abnormalities after cardiac surgery are better explained by atelectasis than by increased permeability oedema. Acta anaesthesiologica Scandinavica 2005;49:1302-10.
35. Barnas GM, Campbell DN, Mackenzie CF, Mendham JE, Fahy BG, Runcie CJ, Mendham GE. Lung, chest wall, and total respiratory system resistances and elastances in the normal range of breathing. The American review of respiratory disease 1992;145:110-3.

FIGURE LEGENDS

Figure 1. Shape factors and characteristic partial pressures derived from the time (top) and volumetric (bottom) capnograms. P_{aCO_2}: partial pressure of arterial blood CO_2; P_{ACO_2}: mean alveolar CO_2 concentration at the midpoint of phase III of CO_2 expiration; $P_{\bar{E}CO_2}$: mixed partial pressure of CO_2 during the entire expiration; P_{ETCO_2}: end-tidal CO_2 concentration. $S_{II,T,V}$: phase II slope of the time and volumetric capnogram, respectively. $S_{III,T,V}$: phase III slope of the time and volumetric capnogram, respectively. D_{2min} and D_{2Vmin}: curvature at the phase II-III transitions, calculated as the minimum of the second-order time and volumetric derivative, respectively. α_{cap}: angle formed by the phase-II and phase-III limbs of the expiratory time capnogram.

Figure 2. Resistive (Raw: airway resistance, R_{vent}: total lung resistance displayed by the ventilator, RL: total lung resistance obtained by oscillometry, Rti: tissue resistance obtained by oscillometry) and elastic lung mechanical parameters (C_{vent}: compliance displayed by the ventilator, CL: compliance determined by oscillometry) and expiratory flow indices (PF: peak flow, LF: late flow) before and after the cardiopulmonary bypass (CPB). *: $p<0.05$ before vs. after the CPB. Values are expressed as mean±SEM.

Figure 3. Indices derived from the time and volumetric capnographic measurements before and after the cardiopulmonary bypass (CPB). $S_{II,T,V}$ and $Sn_{II,T,V}$: absolute and normalized phase-II slopes of the time and volumetric capnogram, respectively. $S_{III,T,V}$ and $Sn_{III,T,V}$: absolute and normalized phase-III slopes of the time and volumetric capnogram, respectively. D_{2min} and D_{2Vmin}: curvature at the phase II-III transitions, calculated as the minimum of the second-order time and volumetric derivative, respectively. V_{DF}, V_{DB} and V_{DE} denote dead-spaces according to Fowler, Bohr and Enghoff. Qs/Qt: intrapulmonary shunt blood flow. Values are expressed as mean±SEM.

Figure 4. Strengths of correlations between the lung mechanical parameters (x-axis) and those obtained by time and volumetric capnography, reflecting the absolute and normalized slopes, and the absolute values reflecting transitions, dead-space and shunt fractions (y-axis). The sizes of the circles denote the magnitude of the Pearson correlation coefficient. Open circles: significant positive correlation; closed circles: significant negative correlation; no circles: no significant correlation.

Figure 5. Strengths of correlations between the fundamental lung mechanical parameters (Raw and C_{vent}; x-axis) and phase II and III slopes obtained by time capnography (y-axis). Panel A: correlations between initial absolute values in the whole population (Pooled) and in subgroups with 25 percentile low and high initial HQ levels. Panel B: correlations between the changes in these parameters for the whole population (Pooled) and in subgroups with the highest 25 percentile increase (I_{max}), and lowest 25 percentile decrease (D_{max}) in HQ after surgery. The sizes of the circles denote the magnitude of the Pearson correlation coefficient. Open circles: significant positive correlation; closed circles: significant negative correlation; no circles: no significant correlation.

Figure

Click here to download Figure Fig-2.PDF

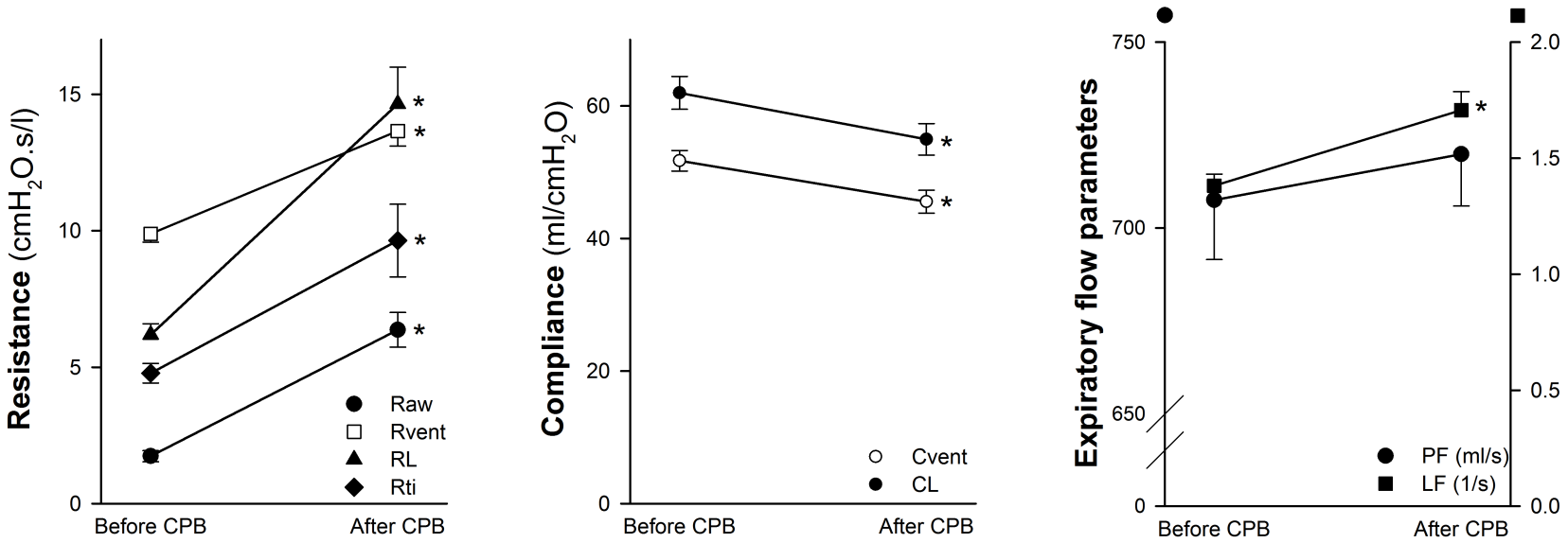

Figure 2

Figure

Click here to download Figure Fig-3.PDF

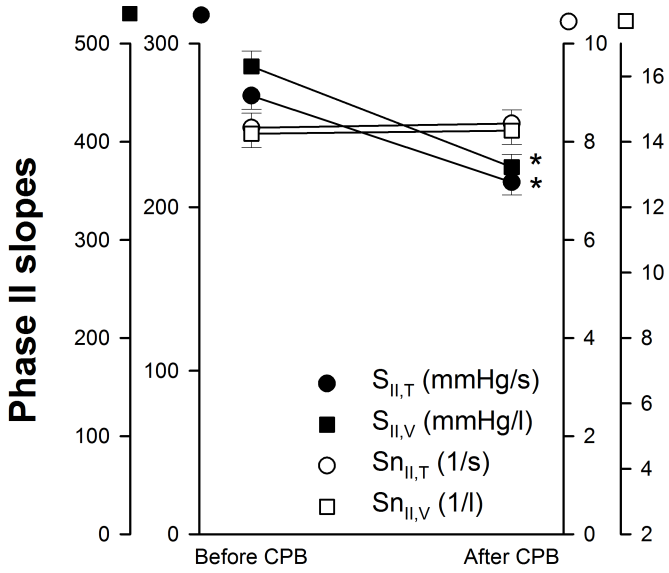

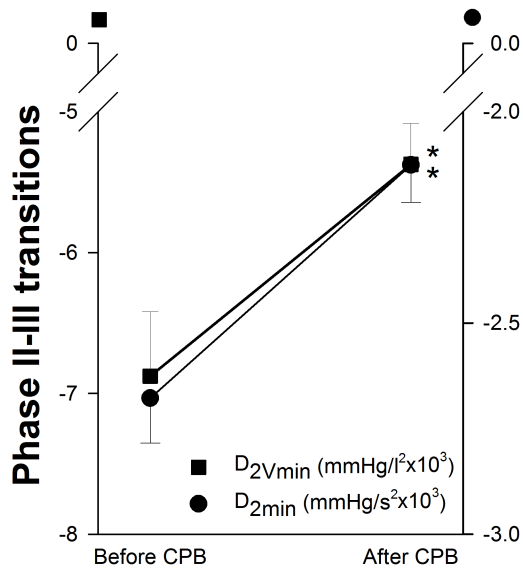

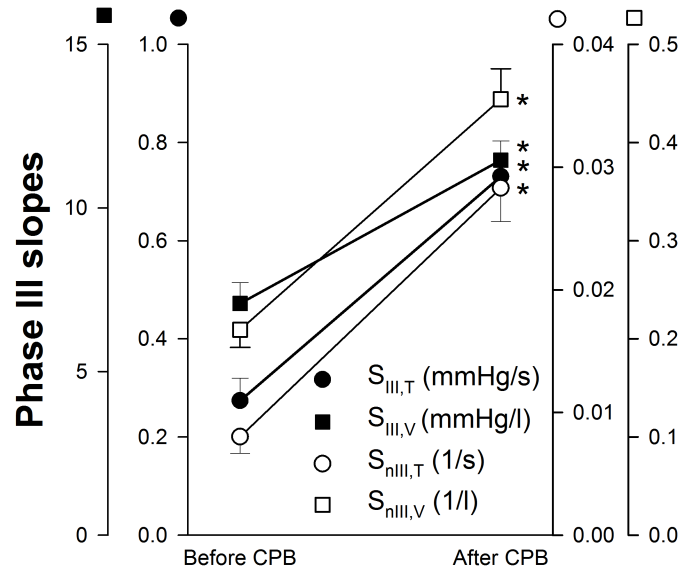

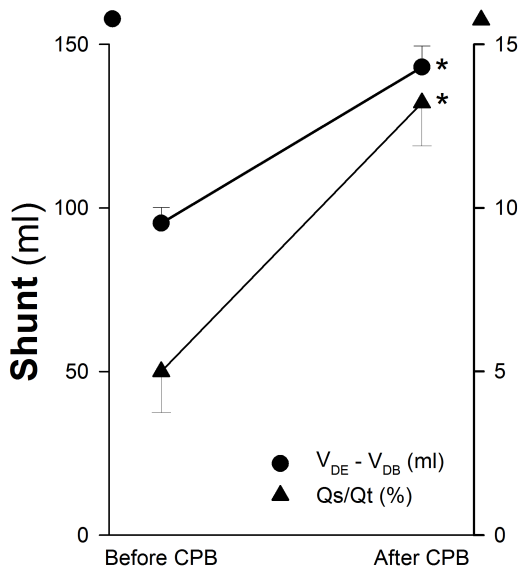

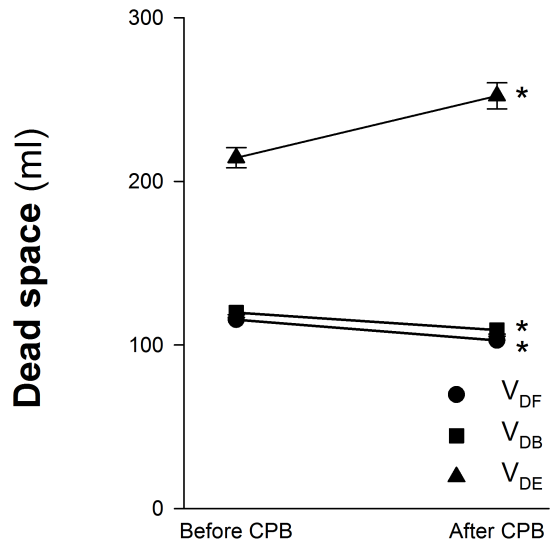

Figure 3

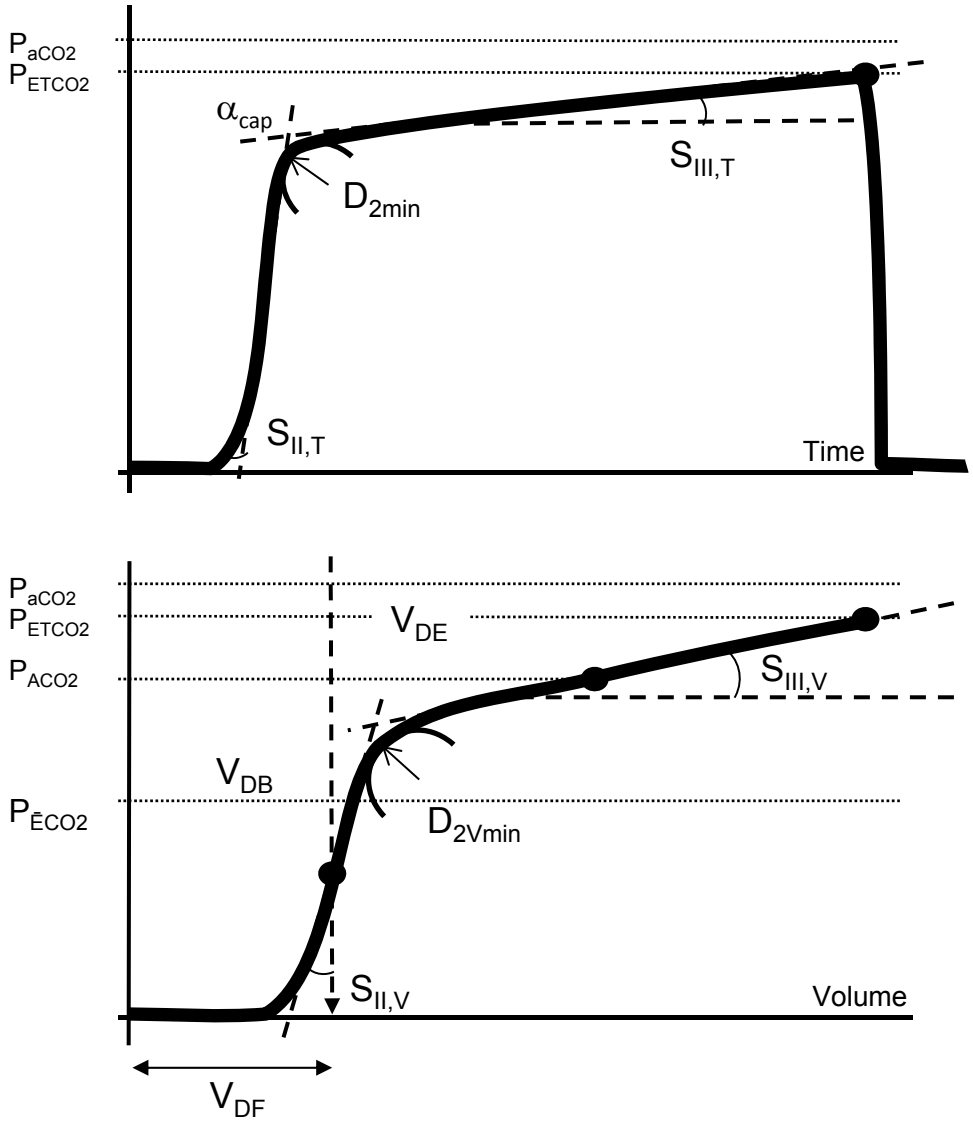

Figure 1

Figure

Click here to download Figure Fig-4-R2.pdf

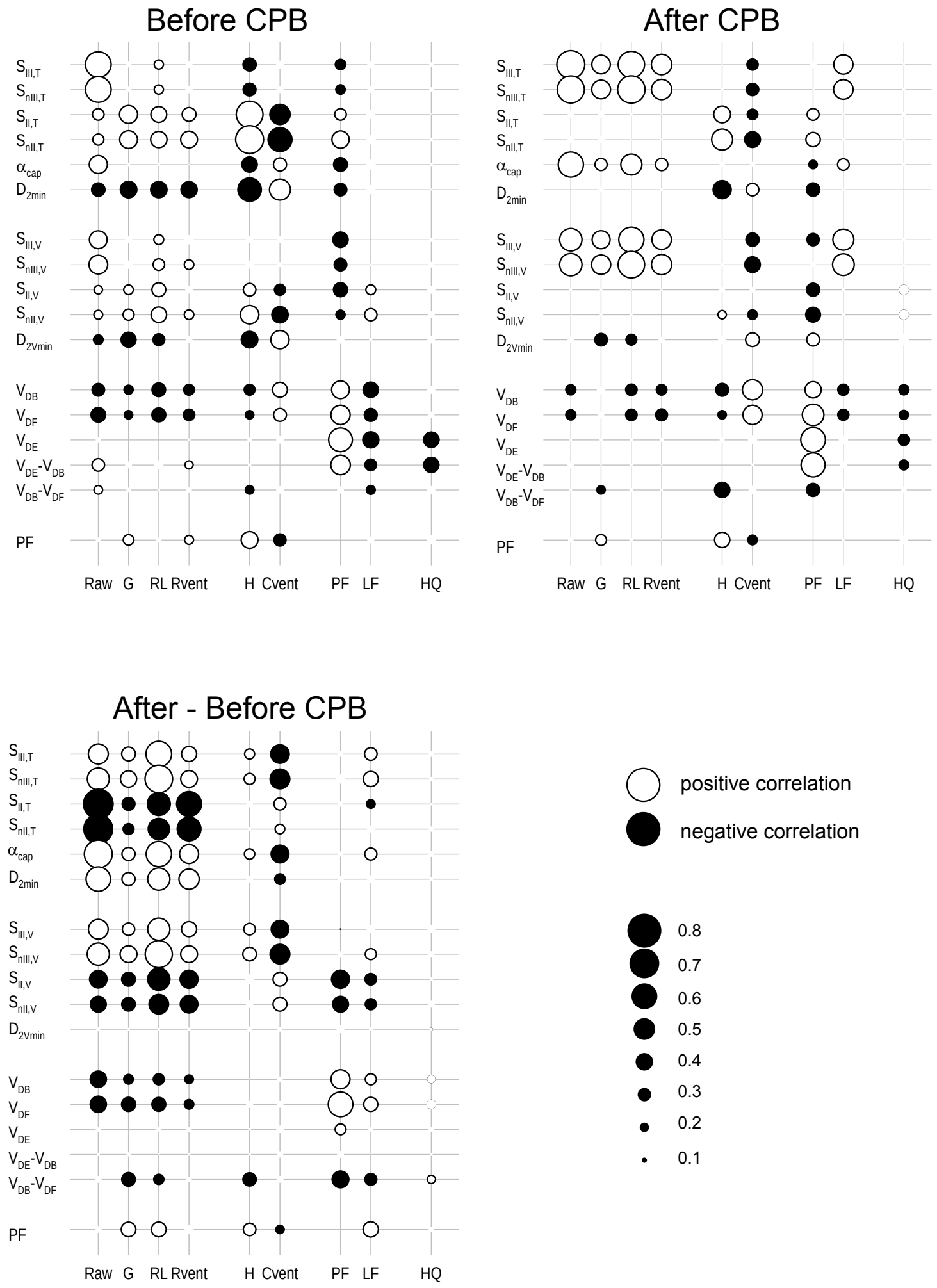

Figure 4

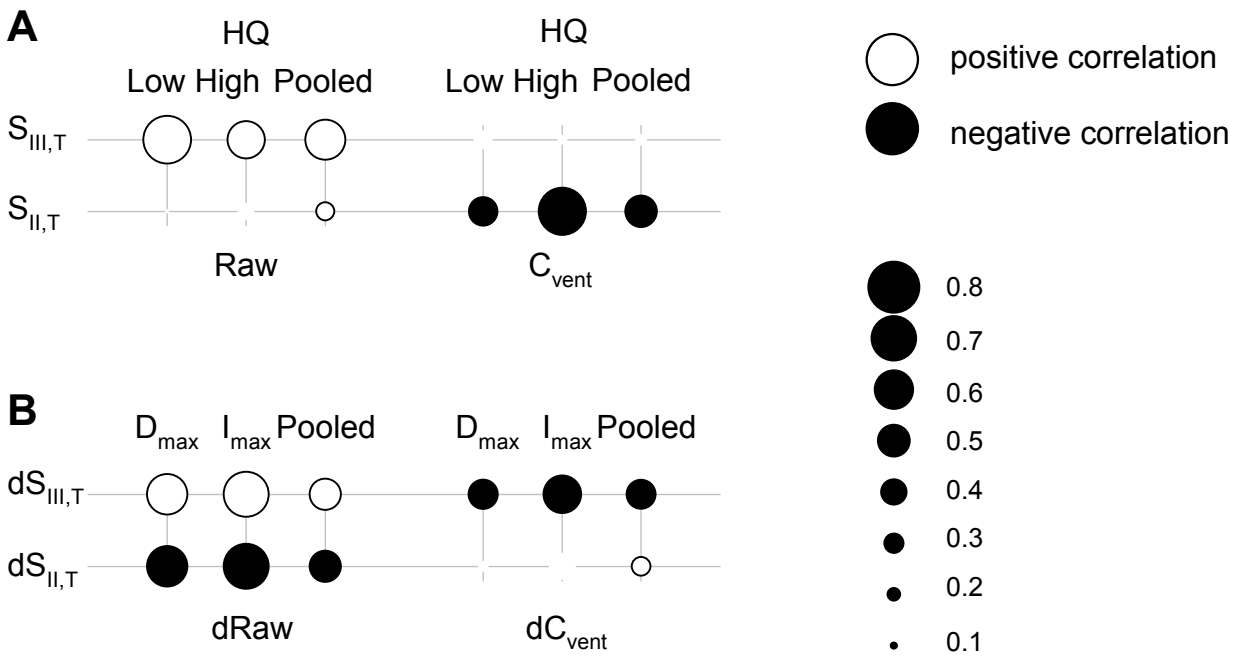

Figure 5